WILEY-VCH

In Situ Analysis of Membrane-Protein Binding Kinetics and Cell–Surface Adhesion Using Plasmonic Scattering Microscopy

Pengfei Zhang,[a] Xinyu Zhou,[a][b] Jiapei Jiang,[a][b] Jayeeta Kolay,[a] Rui Wang,[a] Guangzhong Ma,[a] Zijian Wan,[a][c] and Shaopeng Wang*[a][b]

[a]   Dr. P. Zhang, Mr. X. Zhou, Mr. J. Jiang, Dr. J. Kolay, Dr. R. Wang, Dr. G. Ma, Mr. Z. Wan, Dr. S. Wang
         Biodesign Center for Bioelectronics and Biosensors
         Arizona State University
         Tempe, Arizona 85287, USA
         E-mail: Shaopeng.Wang@asu.edu
[b]   Mr. X. Zhou, Mr. J. Jiang, Dr. S. Wang
         School of Biological and Health Systems Engineering
         Arizona State University
         Tempe, Arizona 85287, USA
[c]   Mr. Z. Wan
         School of Electrical, Energy and Computer Engineering
         Arizona State University
         Tempe, Arizona 85287, USA

Abstract: Surface plasmon resonance microscopy (SPRM) is an excellent platform for in situ determining membrane protein binding kinetics and cell-substrate interactions. However, SPRM suffers from a poor spatial resolution and small field of view, preventing its wide applications. Herein, we demonstrate plasmonic scattering microscopy (PSM) by adding a dry objective on a popular prism-coupled surface plasmon resonance system. PSM not only retains SPRM's high sensitivity and real-time analysis capability to quantify binding kinetics, but also provides ~7 times higher spatial resolution and ~70 times larger field of view than the classical SPRM, thus providing more credible information about the cell-substrate contacts and more details about cellular membrane response to ligand binding on over 100 cells simultaneously. In addition, the PSM also maintains the high sensitivity of SPRM in quantifying the target movements in the axial direction, thus allowing mapping of the adhesion spring constants, which can be used for quantitatively describing the mechanical properties of the cell-substrate interactions, by statistically analyzing the thermal motion characteristics at each pixel. This work may offer a powerful and cost-effective strategy for upgrading current SPR products for studying membrane protein binding kinetics and cell-substrate interactions in detail.

Table of Contents

Experimental Procedures

1. Materials

WGA (Cat. No. L0636) and acetylcholine chloride (Cat. No. A2661) were purchased from Sigma-Aldrich. Anti-EGFR (Cat. No. 05-101) monoclonal antibody and 0.1% gelatin solution (Cat. No. ES-006-B) were purchased from the EMD Millipore. The storage buffer for the proteins were removed with Zeba spin desalting columns (Cat. No. 89882, ThermoFisher) before experiments. PBS buffer (Cat. No. 21-040-CV) and 25-cm^2 flask (Cat. No. 3289) were purchased from Corning. Live cell imaging solution (Cat. No. A14291DJ), DiI cell labeling solution (Cat. No. V22889), fetal bovine serum (Cat. No. 10437036), and Trypsin-EDTA (0.05%, Cat. No. 25300120) were purchased from ThermoFisher. The fetal bovine serum was inactivated by heating to 56 °C for 30 minutes. Penicillin-streptomycin mixture (Cat. No. DE17-602F) was purchased from Lonza. Dulbecco's Modified Eagle's Medium (DMEM, Cat. No. 20-2002) and Eagle's Minimum Essential Medium (EMEM, Cat. No. 30-2003) were purchased from ATCC. 0.9-cm^2 flexi-perm silicon chamber was purchased from the Sarstedt. 4% paraformaldehyde in PBS (Cat. No. J61899) was purchased from Alfa Aesar. BK7 cover glass (Cat. No. 48366-067) was purchased from VWR. Gold-coated glass slides were fabricated by coating a BK7 glass cover slides with 1 nm of Cr followed by 47 nm of gold via thermal evaporation (PVD75 E-beam/Thermal Evaporator, Kurt J. Lesker Company). Before coating, the gold surface was rinsed by ethanol and deionized water twice.

2. Cell Culture

The A431, HeLa, and RBL-2H3 cells were purchased from ATCC. The SH-EP1 wild type (SH-EP1 WT) and SH-EP1 α4β2 cells were gifts from Dr. Jie Wu[1]. All the cells were cultured in a 25-cm^2 flask at 37 °C with 5% CO_2 and 70% relative humidity. The A431 and HeLa cells were grown in DMEM with 10% fetal bovine serum and 1% penicillin-streptomycin mixture. The RBL-2H3 cells were grown in EMEM with 15% fetal bovine serum and 1% penicillin-streptomycin mixture. The SH-EP1 cells were grown in EMEM with 10% fetal bovine serum and 1% penicillin-streptomycin mixture. Cells were passaged with 0.05% Trypsin-EDTA when they were approximately 80% confluent. Before attaching the cells to the sensor surface, ~600 µL gelatin solution was added to the flexi-perm silicon chamber on the gold-coated glass slide, and then incubated in the incubator at 37 °C. Then, the gelatin solution was removed, and the gold-coated glass slides were dried naturally in the bio-hood. After waiting for ~4 hours after drying, ~10000 cells were added to each flexi-perm silicon chamber. For fixing cells, the cells were incubated in 4% paraformaldehyde in PBS for 10 min at room temperature and then rinsed with PBS buffer.

3. Optical Imaging Setup

The SPRM is constructed in an inverted microscopy (Olympus IX81) as described before[2]. The large view PSM was constructed on a SPR imaging system. Light from a laser diode with center wavelength of 660 nm (Coherent OBIS LX 660 nm 75 mW Laser System, Fiber Pigtail, FC) was conditioned by three lenses configured in a 4-f arrangement, and then excite the SPR on the gold coated glass slide placed on a prism (Cat. No. 49431, Edmund optics). The scattered surface plasmonic waves were collected by a 10x dry objective (Motic), and imaged by a USB 3.0 CMOS camera (XIMEA MC124MG-SY). A quartz tungsten-halogen lamp (QTH100, Thorlabs) was employed as the illumination for bright field imaging. The flow cells were constructed as described before[3]. More detailed schematic representation of the optics can be found in Fig. S1.
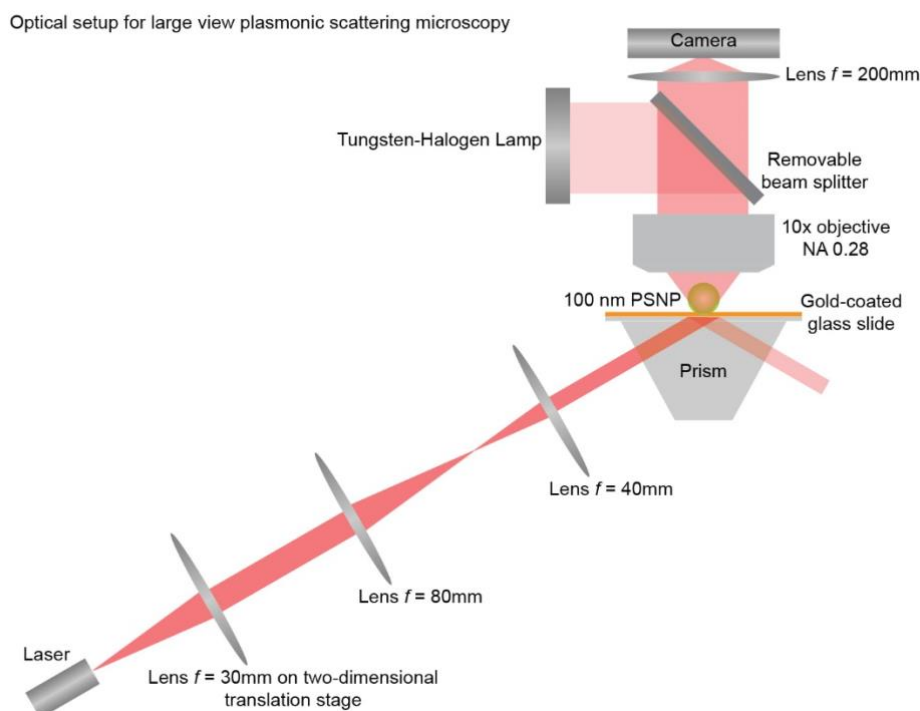

Figure S1. Optical setup for large view plasmonic scattering microscopy. Light from a laser diode with a center wavelength of 660 nm (Coherent OBIS LX 660 nm 75 mW Laser System, Fiber Pigtail, FC) was conditioned by three lenses configured in a 4-f arrangement. Three lenses have the focus length of 30 mm, 80 mm and 40 mm, respectively. The distance between laser and first lens, between first and second lens, between second and third lens, and between third lens and prism surface are set to be 30 mm, 110 mm, 120 mm and 40 mm to construct the 4-f arrangement. The 4-f arrangement allows scanning the incident angles without changing the illumination area. The illumination area has the ellipse shape with a size of ~1.8 mm × 1.2 mm due to the oblique illumination configuration. The scattering of surface plasmonic waves by analytes was collected by a Motic 10 x objective on the top of gold-coated glass slide, and then imaged by the camera (XIMEA MC124MG-SY). A tungsten-halogen lamp was used as the light source for bright field imaging, and the beam splitter was inserted to construct the bright field imaging path. It should be noted that the beam splitter will be removed during PSM imaging processes to avoid reducing the signal intensity.

4. Simultaneous SPR and PSM imaging of cells

Putting one Olympus LCPlanFLN 100X objective (numerical aperture of 0.85) on the top of one classical SPRM can allow simultaneous SPR and PSM imaging[3]. Without the collection of strong reflection and interference among delocalized plasmonic waves, the PSM can provide higher spatial resolution and better image contrast than classical SPRM. In addition, the high numerical aperture objective can show more details than the low numerical aperture objective but with a smaller field of view. The selection of observation objective is a trade-off between the throughput and spatial resolution.
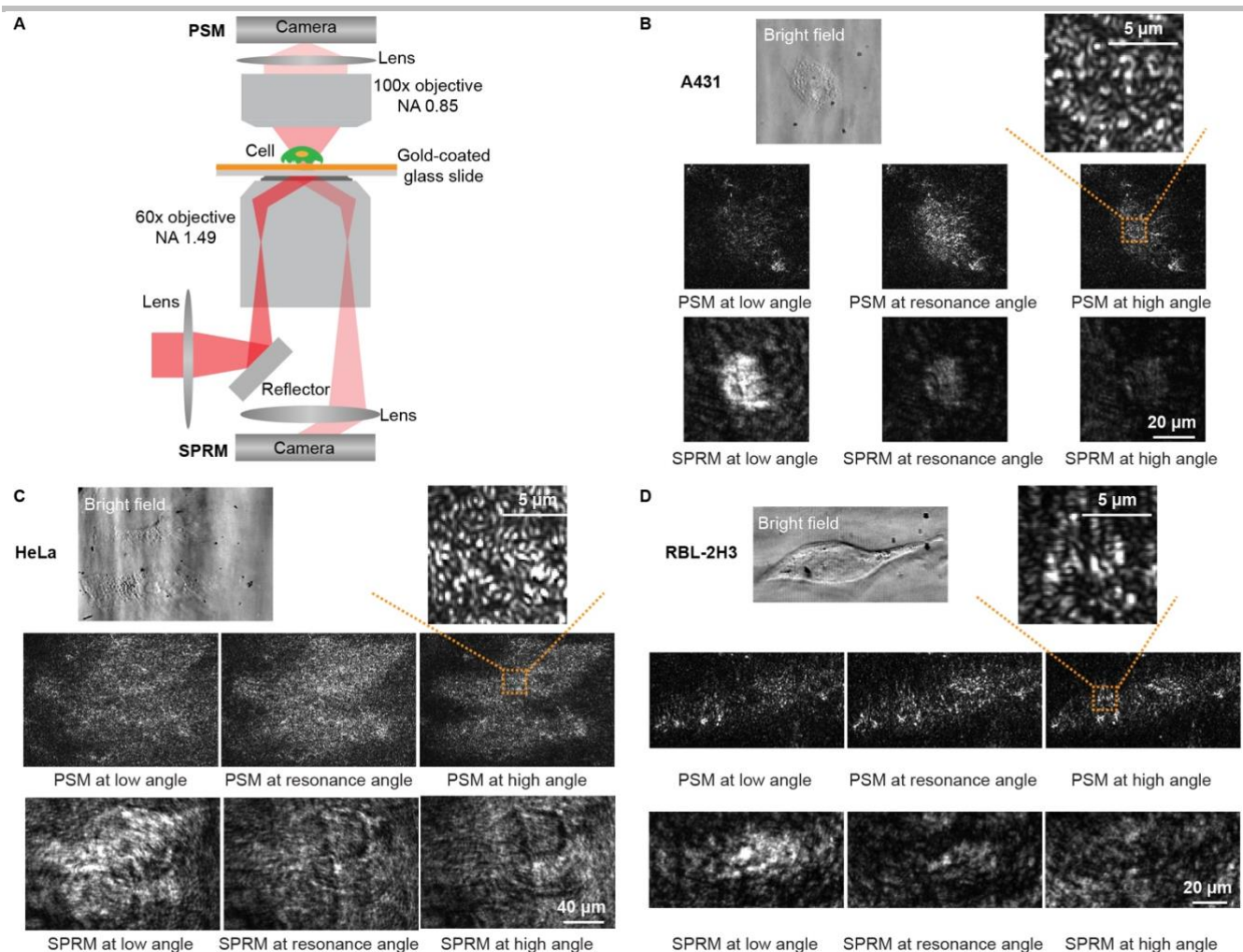
Figure S2. Simultaneous SPR and PSM imaging of cells. (A) Schematic of the optical setup. (B), (C), and (D) Simultaneous SPR and PSM imaging of fixed A431(B), HeLa(C), and RBL-2H3(D) cells at different incident angles.

5. PSM and TIRF imaging

The A431, HeLa, and RBL-2H3 cells were incubated in 10 µM DiI in a culture medium for 1 hour, and then fixed with immersion in 4% paraformaldehyde in PBS for 10 minutes. Then, the cells were washed with PBS buffer three times, and placed in the system for scattering and total internal reflection fluorescence (TIRF) imaging. Coherent OBIS LX 660 nm 75 mW laser was employed for scattering imaging. Coherent OBIS LS 532 nm 120 mW laser, Thorlabs DMSP550R short pass dichroic mirror with a cutoff wavelength of 550 nm, and Thorlabs FGL570M long pass filter with a cut-on wavelength of 570 nm were employed for TIRF imaging.

Fig. S3 shows the PSM and TIRF imaging of A431, HeLa, and RBL-2H3 cells on gold-coated glass slides. Fig. S4 shows the evanescent scattering and TIRF imaging of A431, HeLa, and RBL-2H3 cells on conventional cover glasses, where the evanescent wave created by total internal reflection was employed to replace the surface plasmonic wave to avoid the fluorescence quenching effect of the gold film. After comparing the scattering images with TIRF images, we can see similar morphologies in both PSM and TIRF images, which indicate that the scattering signals should mainly come from the membrane-substrate contacts, even on the gold film with a quenching effect. Some bright spots, which can only be observed by scattering imaging, may come from the high refractive index cellular vesicles or other similar organelles nearby the cellular membrane[4].
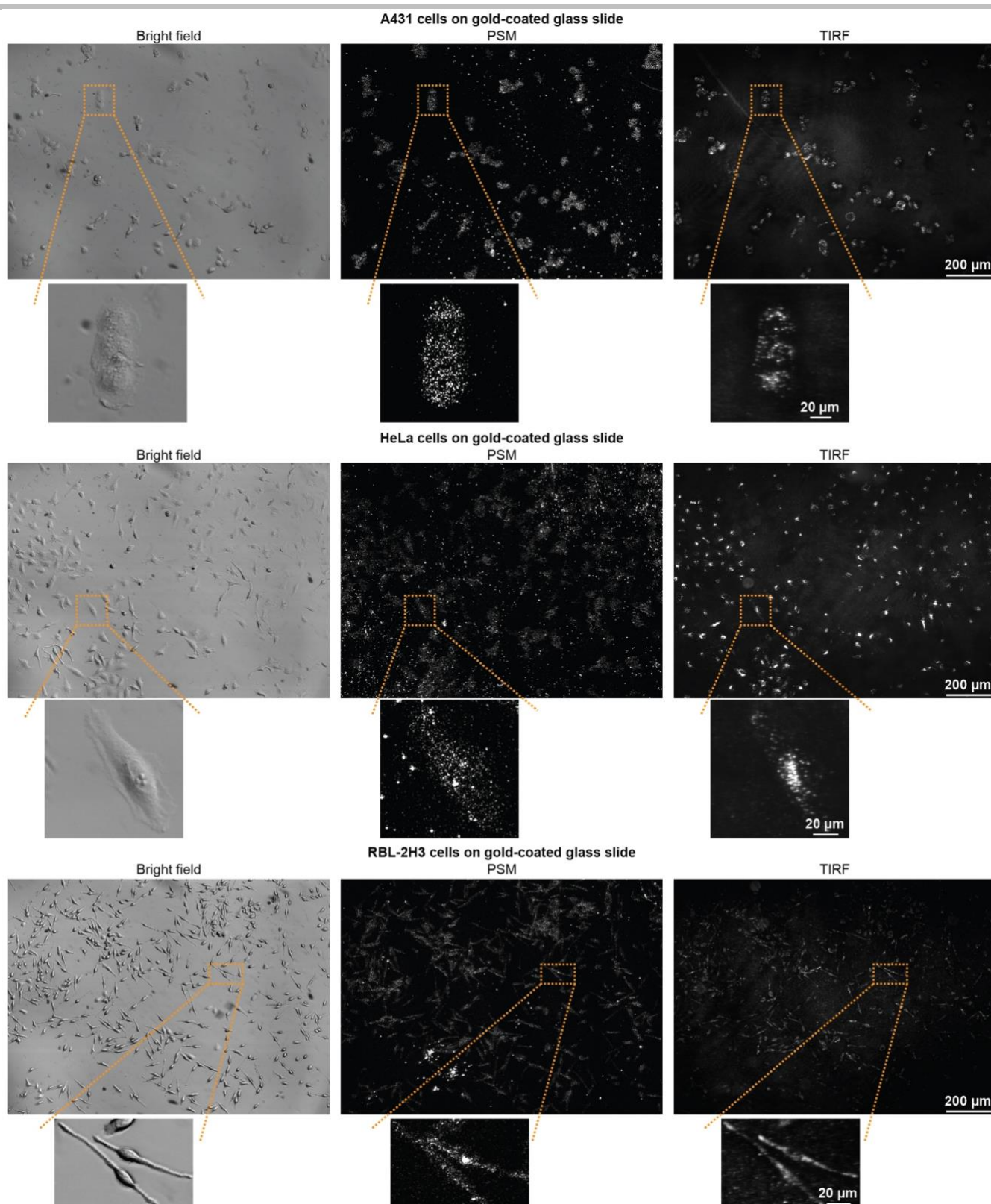
SUPPORTING INFORMATION

Figure S3. PSM and TIRF imaging of cells. The cells were incubated and fixed on gold-coated glass slides. The incident intensity and camera exposure time are 3 W/cm^2 and 50 ms for PSM images, 10 W/cm^2 and 300 ms for TIRF images.
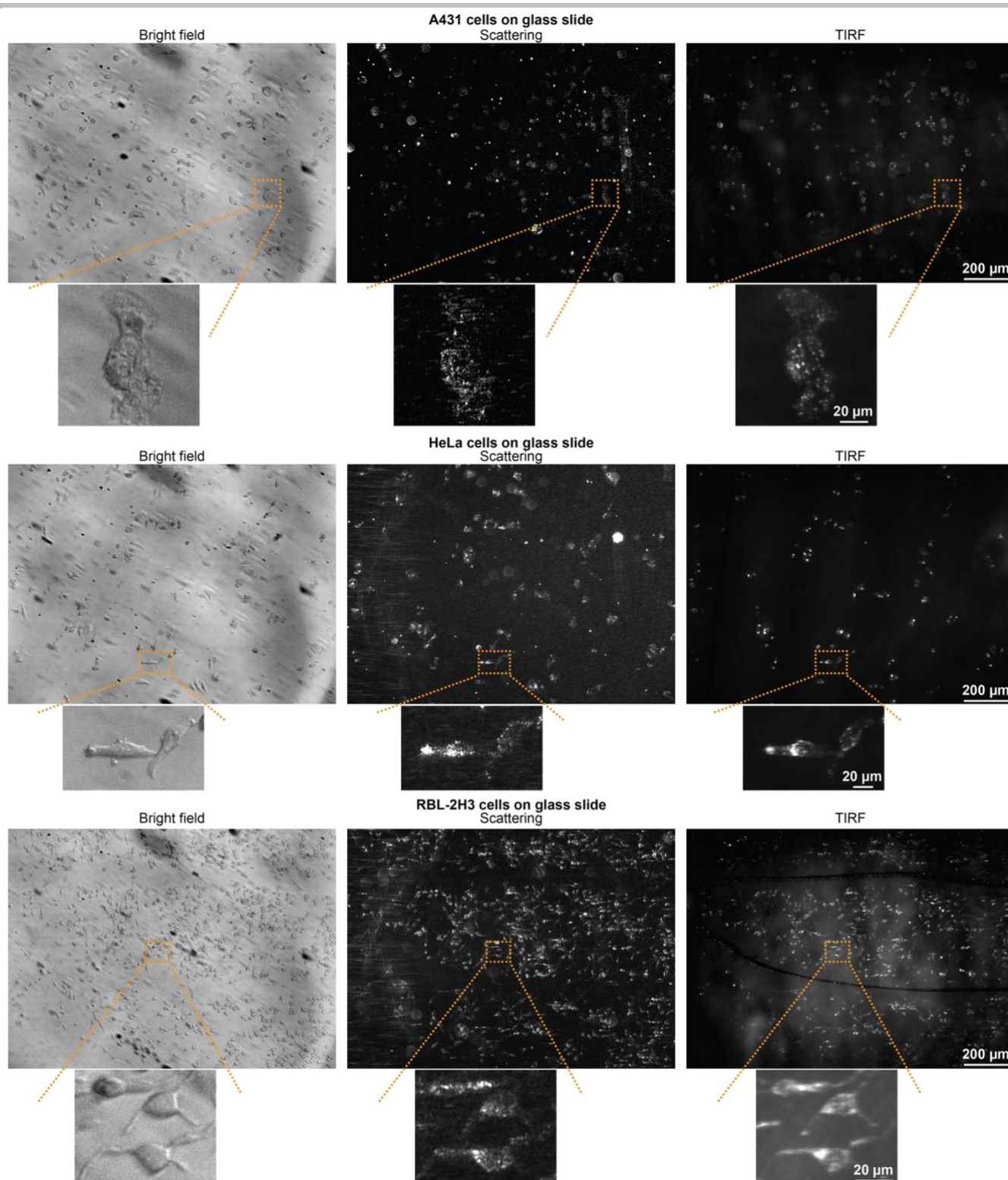
SUPPORTING INFORMATION

Figure S4. Evanescent scattering and TIRF imaging of cells. The cells were incubated and fixed on conventional cover glasses. The incident intensity and camera exposure time are 3 W/cm^2 and 300 ms for evanescent scattering images, 10 W/cm^2 and 100 ms for TIRF images.

6. Data analysis

The PSM images for the cells were recorded with exposure time of 50 ms and rate of ~17 frames per second (fps), which is limited by the camera. The image sequence was averaged by XIMEA Camtool software by 4 frames to reduce the data size, and thus the effective frame rate is ~4.2 fps. The ROI manager of ImageJ Fiji was employed to select the cell adhesion area, and the Plot Z-axis Profile plugin was used to achieve the image intensity variation along with the time. Scrubber v.2.0a was used to determine the association and dissociation rate constants by fitting the curves with the first-order binding kinetics model. For estimating the cell adhesion areas shown in Fig. 5, the TrackMate plugin of ImageJ Fiji was used to achieve the locations of all bright spots created by adhesion sites, averaging the locations of 50 bright spots at two ends in one direction, and then subtract two averaged locations to achieve the length of one ellipse axis. Following similar procedure, the length of the other ellipse axis can be achieved, and then the ellipse area can be estimated with area formula.

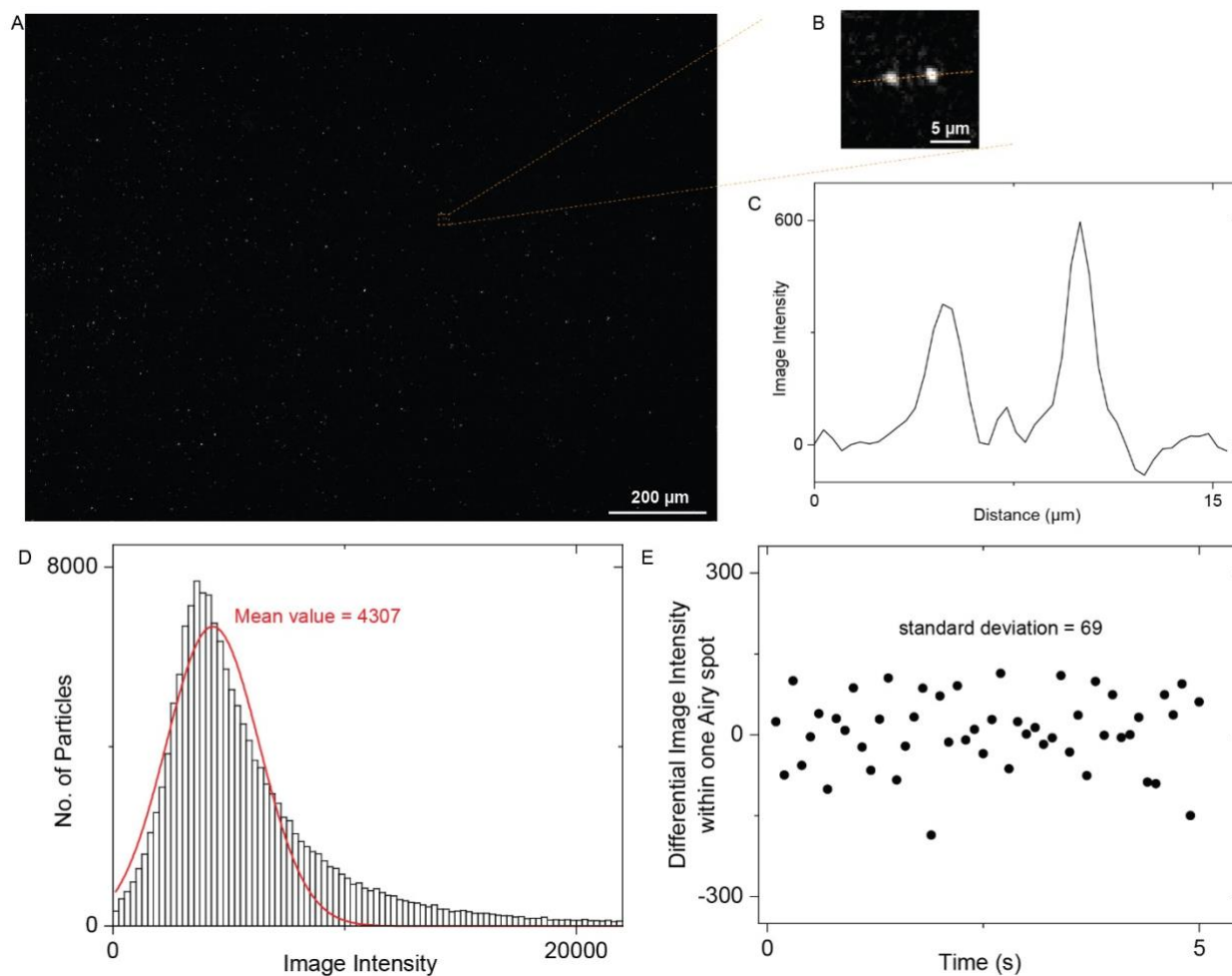## 7. PSM imaging of 100 nm polystyrene nanoparticles

Figure S5. (A) A PSM image of 100 nm polystyrene nanoparticles binding to the bare gold film surface. (B) Zoomed view of the marked zone in (A). (C) Profile of the line marked in (B). (D) Image intensity histograms of 100 nm polystyrene nanoparticles binding to the bare gold within 3 minutes. The image intensity is achieved by integrating the intensities of all pixels within the Airy disk at the nanoparticle binding site. (E) Total image intensity fluctuations in an Airy disk without binding within 5 seconds. The signal-to-noise ratio of PSM measurement of 100 nm polystyrene nanoparticles can be estimated to be 4307/69 ~ 62. The detailed procedure for measuring the binding of polystyrene nanoparticles has been described before[4].

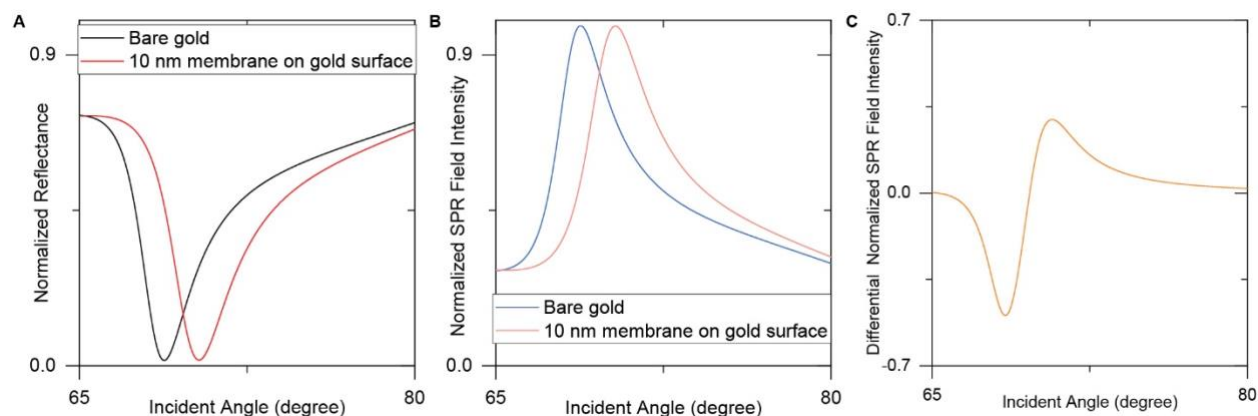## 8. Simulation of PSM image intensity against incident angle

Figure S6. Simulation of PSM image intensity against incident angle. (A) SPR simulation for reflectivity versus incident angle on bare gold (black) and cell membrane (red) with Winspall data analysis software (http://res-tec.de/downloads.html). The thickness of cell membrane attached on the gold surface was estimated to be 10 nm. (B) The intensity of surface plasmonic wave is reversely related to the reflection intensity, and thus the PSM intensity curve can be achieved by reversing the SPR resonance curves shown in (A). (C) Differential curve achieved by subtracting the membrane curve with bare gold curve shown in (B), showing that the PSM intensity response to additional analyte binding can be negative, zero and positive.

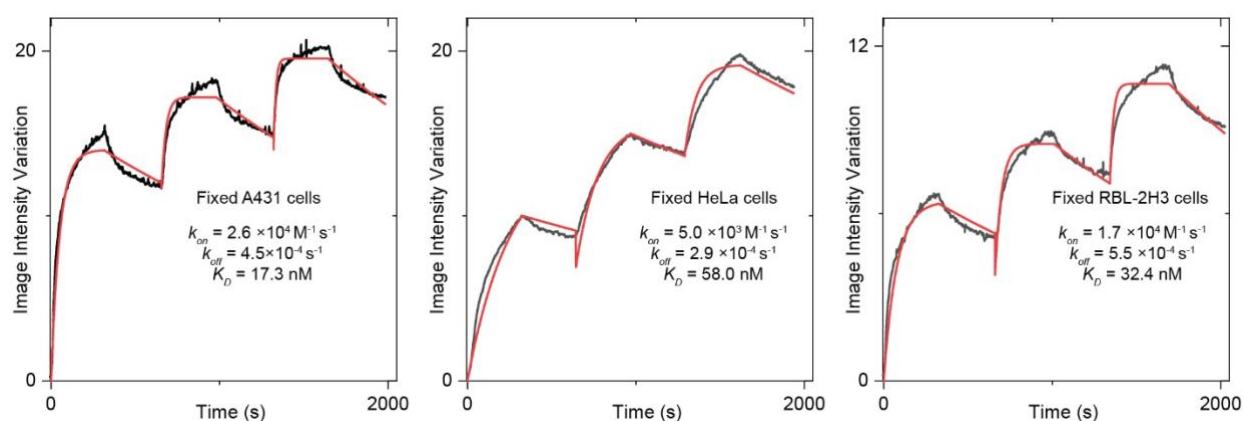## 9. Fixed cell response to WGA with different concentrations

Fixed A431 cells
k_{on} = 2.6 ×10^4 M^{-1}s^{-1}
k_{off} = 4.5×10^{-4} s^{-1}
K_D = 17.3 nM

Fixed HeLa cells
k_{on} = 5.0 ×10^3 M^{-1}s^{-1}
k_{off} = 2.9×10^{-4} s^{-1}
K_D = 58.0 nM

Fixed RBL-2H3 cells
k_{on} = 1.7 ×10^4 M^{-1}s^{-1}
k_{off} = 5.5×10^{-4} s^{-1}
K_D = 32.4 nM

Figure S7. The responses of fixed A431, HeLa, and RBL-2H3 cells to 25, 50 and 100 µg/mL WGA in PBS buffer were measured, and fitted by kinetic titration model without regeneration to avoid destroying the fragile cellular membrane.

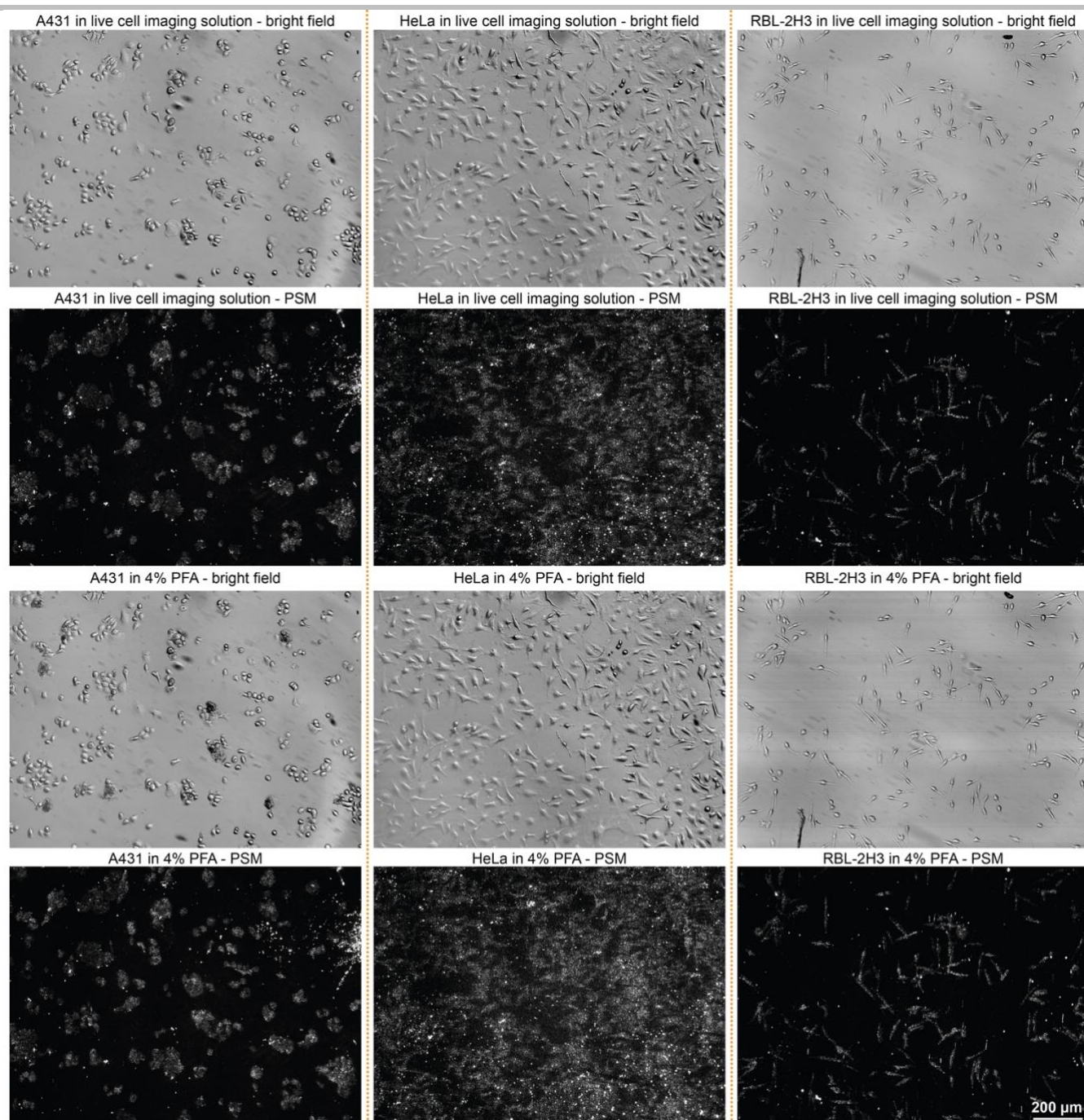## 10. Bright field and PSM images of cells in living and fixed conditions

10

Figure S8. Bright field and PSM images of A431, HeLa, and RBL-2H3 cells in living and fixed conditions.

11. Object motion tracking in the axial direction

Fig. S9A shows the object motion tracking at one pixel as an example. Analyzing the intensity fluctuations can give the time trace of object motion in the axial direction. Then, the statistical analysis of the motion amplitude can give the free energy profiles, and the spring constant can be achieved by fitting the free energy profiles. The detailed calculation approach has been reported previously[3, 5], and the codes have been published at https://doi.org/10.5281/zenodo.6471541.
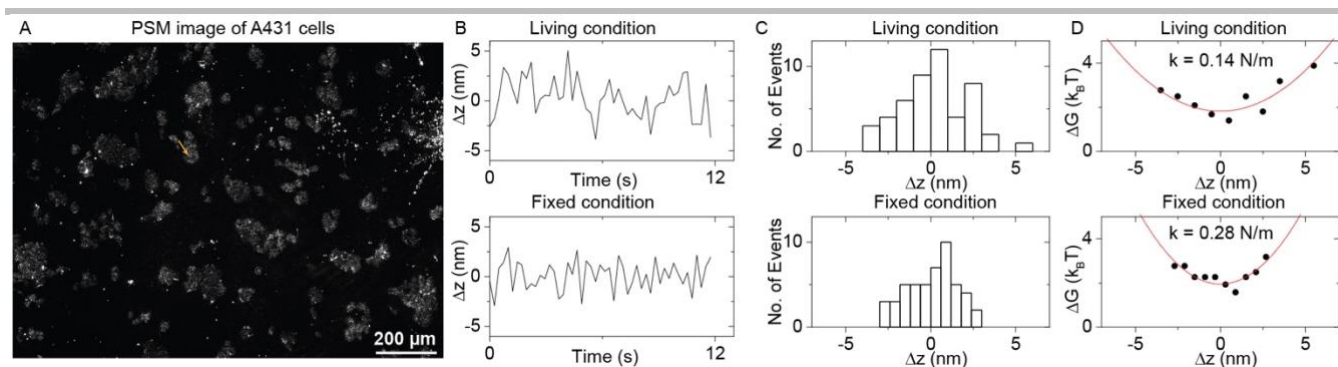
Figure S9. Object motion tracking at a single pixel. (A) A PSM image of A431 cells. (B) Time trace of z-displacement of cell adhesion site in one pixel. (C) Probability density determined from the statistical distribution of z-displacement amplitude. (D) Free energy profile achieved from the probability density and fitted results with a polynomial function. The spring constant obtained from the fitting was also presented.

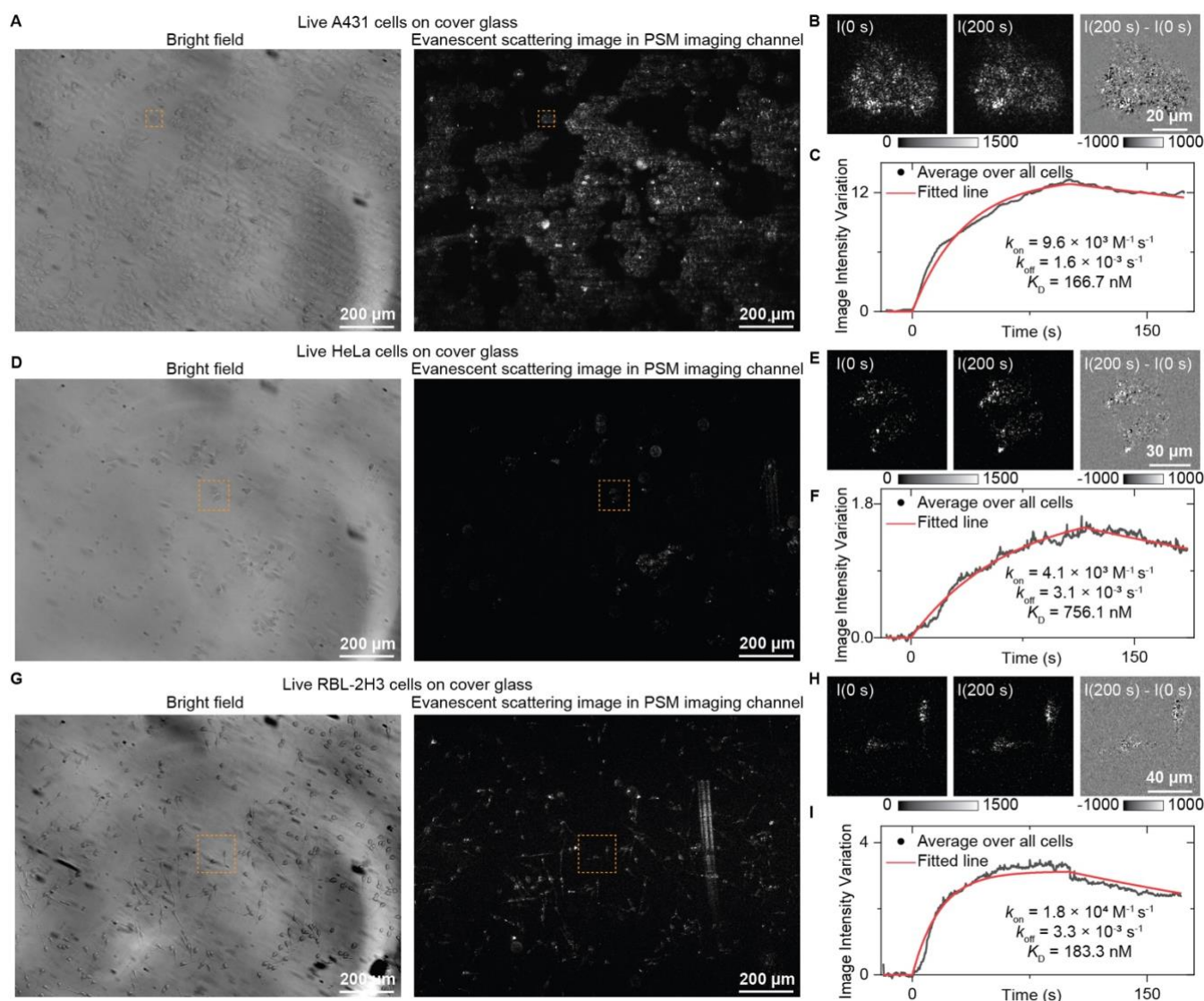## 12. Evanescent scattering imaging of membrane binding kinetics on cover glasses

Figure S10. Evanescent scattering measurement of WGA binding to membrane in live cells on cover glasses. (A, D and G) Bright field and evanescent scattering images of live A431 (A), HeLa (D), and RBL-2H3 (G) cells. (B, E and H) Zoomed views of marked region in (A, D and G) at 0 s and 200 s after changing the flow to 100 µg/mL WGA solution, and the differential image. (C, F and I) The image intensity variation against time by averaging the signal of all cells within the field of view

shown in (A, D and G). The fitted line is achieved by fitting the curve with a first-order binding kinetics model. The incident wavelength, incident intensity, and camera exposure time are 532 nm, 10 W/cm^2, and 50 ms, respectively.

13. Captions for Supplementary Movies

Movie S1.
Comparison of fixed and living A431 cells response to WGA binding in whole field of view.
Movie S2.
Comparison of fixed and living A431 cells response in WGA solution and buffer in a zoomed view.
Movie S3.
Comparison of fixed and living HeLa cells response in WGA solution and buffer in a zoomed view.
Movie S4.
Comparison of fixed and living RBL-2H3 cells response in WGA solution and buffer in a zoomed view.
Movie S5.
Spring constant maps of A431, HeLa, and RBL-2H3 cells against time during the fixing process.

References

[1]   J. Wu, Y.-P. Kuo, A. A. George, L. Xu, J. Hu, R. J. Lukas, J. Biol. Chem. 2004, 279, 37842-37851.
[2]   a) W. Wang, K. Foley, X. Shan, S. Wang, S. Eaton, V. J. Nagaraj, P. Wiktor, U. Patel, N. Tao, Nat. Chem. 2011, 3, 249-255; b) W. Wang, Y. Yang, S. Wang, V. J. Nagaraj, Q. Liu, J. Wu, N. Tao, Nat. Chem. 2012, 4, 846-853.
[3]   P. Zhang, X. Zhou, R. Wang, J. Jiang, Z. Wan, S. Wang, ACS Sensors 2021, 6, 4244-4254.
[4]   Y. Yang, H. Yu, X. Shan, W. Wang, X. Liu, S. Wang, N. Tao, Small 2015, 11, 2878-2884.
[5]   a) H. Wang, Z. Tang, Y. Wang, G. Ma, N. Tao, J. Am. Chem. Soc. 2019, 141, 16071-16078; b) P. Zhang, L. Zhou, R. Wang, X. Zhou, J. Jiang, Z. Wan, S. Wang, Nat. Commun. 2022, 13, 2298.

Author Contributions

Dr. P. Z. and Dr. S. W. designed the research; Dr. P. Z. built the setup and performed the measurement and data analysis; Mr. X. Z., Mr. J. J., Dr. J. K., and Dr. R. W., contributed to the cell culture; Dr. G. M. contributed to the data analysis; Mr. Z. W. and prepared the gold-coated glass slides; Dr. S. W. supervised the experiments; Dr. P. Z., Dr. R. W., Dr. G. M., and Dr. S. W. wrote the paper.